Possible Impacts of Winter Arctic Oscillation on Siberian High, the East Asian Winter Monsoon and Sea–Ice Extent[1]

Wu Bingyi (武炳义)[2]

Institute of Atmospheric Physics, Chinese Academy of Sciences, Beijing 100029

Wang Jia (王 佳)

International Arctic Research Center–Frontier Research System for Global Change, University of Alaska Fairbanks, Alaska 99775

(Received April 17, 2001; revised December 28, 2001)

ABSTRACT

Using the NCEP–NCAR reanalysis dataset covering a 40–year period from January 1958 to December 1997, sea surface temperature (1950–1992), and monthly sea–ice concentration dataset for the period from 1953 to 1995, we investigate connections between winter Arctic Oscillation (AO) and Siberian high (SH), the East Asian winter monsoon (EAWM), and winter sea–ice extent in the Barents Sea. The results indicate that winter AO not only influences climate variations in the Arctic and the North Atlantic sector, but also shows possible effects on winter SH, and further influences EAWM. When winter AO is in its positive phase, both of winter SH and the EAWM are weaker than normal, and air temperature from near the surface to the middle troposphere is about 0.5–2°C higher than normal in the southeastern Siberia and the East Asian coast, including eastern China, Korea, and Japan. When AO reaches its negative phase, an opposite scenario can be observed.

The results also indicate that winter SH has no significant effects on climate variations in Arctic and the North Atlantic sector. Its influence intensity and extent are obviously weaker than AO, exhibiting a 'local' feature in contrast to AO. This study further reveals the possible mechanism of how the winter AO is related to winter SH. It is found that winter SH variation is closely related to both dynamic processes and air temperature variations from the surface to the middle troposphere. The western SH variation mainly depends on dynamic processes, while its eastern part is more closely related to air temperature variation. The maintaining of winter SH mainly depends on downward motion of airflow of the nearly entire troposphere. The airflow originates from the North Atlantic sector, whose variation is influenced by the AO. When AO is in its positive (negative) phase, downward motion remarkably weakened (strengthened), which further influences winter SH. In addition, winter AO exhibits significant influences on the simultaneous sea–ice extent in the Barents Sea.

Key words: Arctic Oscillation (AO), Siberian high, East asian winter monsoon, Sea–ice extent

1. Introduction

The East Asian winter monsoon system is one of the most active components of the global climate system. Climate variability in East Asia has notable impacts on both adjacent regions and the region far away (Lau and Li 1984; Yasunari 1991; Lau 1992; Wang et al. 2000). In winter the robust Siberian high occupies the Asian continent with a strong Aleutian low to its east. The most prominent surface feature of the East Asian winter monsoon is

[1] This work was supported by the National Key Basic Research Program (Grant No.G1998040900), the Frontier Research System for Global Change of Japan and the National Natural Science Foundation of China under Grant No.49905003.

[2] E–mail: wby@mail.iap.ac.cn

characterized by strong northwesterlies along the east flank of the Siberian high and the coast of East Asia except for the South China Sea where northeasterlies prevails (Chen et al. 2000). At 500 hPa there is a broad trough centered about at the longitudes of Japan. In the high troposphere (200 hPa) the dominant feature is the East Asian jet with its maximum appearing just southeast of Japan. The jet is closely associated with intense baroclinicity, large vertical wind shear, strong advection of cold air, and further with pressure surges.

With respect to some effective factors on the East Asian winter monsoon and Siberian high, the question has received less attention. Many studies have been conducted to explore the relationships between ENSO events and climate variability over East Asia. Some results have revealed that the mature phase of ENSO often occurs in boreal winter and is normally accompanied by a weaker–than–normal winter monsoon along the East Asian coast (Zhang et al. 1996; Tomita and Yasunari 1996; Ji et al. 1997). Consequently, climate in southeastern China and Korea is warmer and wetter than normal during ENSO winter (Tao and Zhang 1998; Wang et al. 2000). Wang et al. (2000) put forwarded that the key system that bridges the warm (cold) events in the eastern Pacific and the weak (strong) East Asian winter monsoon is an anomalous lower–troposphere anticyclone (cyclone) located in the western North Pacific. Thus, they mainly emphasize extratropical–tropical interactions to explain relationship between ENSO events and the East Asian winter monsoon.

Walker (1923) noted a tendency toward simultaneous strengthening or weakening of the Icelandic Low and the Azores high, and first named it the North Atlantic Oscillation (NAO). Since then, problems related to the NAO have been continuously examined. Particularly in the Climate Variability and Predictability (CLIVAR) program, the NAO is an atmospheric factor affecting oceanic variation.

Actually, the NAO represents a teleconnection pattern on sea level pressure (SLP). In order to describe the pattern's strength variation, the NAO index is generally defined as the normalized SLP difference between Ponta Delgada (Azores) and Akureyri (Iceland) (Serreze et al. 1997). The NAO exists throughout a year, and it is most pronounced during the Northern winter. Some studies (Barnston and Livezey 1987) indicate that the NAO variation can account for more than one–third of the total variance of SLP field over the North Atlantic. Moreover, the NAO has been associated with various climatic signals. Hurrell and Van Loon (1997) believe that in addition to the Southern Oscillation, the NAO is a major source of interannual variability of weather and climate around the world; and it is closely associated with changes in the surface westerlies across the North Atlantic into Europe (Hurrell 1995). Furthermore, the NAO contributes to the largest fraction of the Northern Hemisphere temperature variability of any mid–latitude (Hurrell 1996).

Thompson and Wallace (1998) first proposed the concept of the Arctic Oscillation (AO). Some studies have been followed up to investigate AO–related research works (Wang and Ikeda 2000; Fyfe et al. 1999; Skeie 2000; and many others). During a winter, AO's vertical structure extends deep into the stratosphere. Similar findings have also been recognized in the context of troposphere–stratospheric coupling (Baldwin et al. 1994; Perlwitz and Graf 1995; Kitoh et al. 1996; Kodera et al. 1996).

Actually, the NAO and AO are nearly indistinguishable (Dickson et al. 2000), particularly in winter. The AO time series is nearly indistinguishable from the leading structure of variability in the Atlantic sector (e.g. the NAO). Their temporal correlation is 0.95 for monthly SLP anomalies during November–April 1947–97 (Deser 2000).

Since Walker (1923) first put forwarded the concept of the NAO, many researchers focus their attention on the North Atlantic sector to examine some associations of the NAO with a broad range of physical and biological responses in the North Atlantic. Those include variations in wind speed, latent and sensible heat flux (Cayan 1992a, b, c), evaporation–precipitation (Cayan and Reverdin 1994; Hurrell 1995), sea surface temperature (Cayan 1992c; Hansen and Bezdek 1996), and the strength of the Labrador Current (Myers et al. 1989).

Up to now, the relationships between the NAO (AO) and the Siberian high and the East Asian winter monsoon are not well known, although Rogers (1984) suggested that the NAO are associated with significant SLP differences over much of the hemisphere except for Siberia and western North America. Therefore, the associations between winter NAO (AO) and Siberian high, the East Asian winter monsoon have not been understood yet.

Many previous studies investigated Arctic sea–ice variability (Walsh and Johnson 1979; Wang et al. 1994; Wang et al. 1995; Mysak et al. 1996; Slonosky et al. 1997; Mysak and Venegas 1998; Wang and Ikeda 2000; Dickson et al. 2000). Those studies demonstrated clearly that Arctic sea–ice variations get directly tied with the NAO or AO. Previous studies, however, do not stress the causes and possible mechanisms for interannual variations of winter sea–ice extent in the Barents Sea (The study by Dickson et al. (2000) did not explore the reasons for interannual variations of winter sea–ice in the Barents Sea.). Actually, winter sea–ice variations in the Barents Sea are closely associated with climate variations in East Asia on interannual and decadal timescales. A series of preliminary studies of Arctic sea–ice anomalies in the Barents and Kara Seas in conjunction to ENSO events and climate variations over East Asia were conducted by Wu et al. (1997), Wu et al. (1999), and Gao and Wu (1998). In this study, a sea–ice extent index is calculated in the region from 20 to 70°E and south of 82°N.

The purpose of the present study is to examine the question of how the AO in winter affect winter Siberian high, the East Asian winter monsoon, and sea–ice extent in the Barents Sea. We will discuss possible mechanisms for AO influencing Siberian high. For this purpose, in section 2 we first introduce the dataset used, definitions of some atmospheric circulation indices and analysis methods. Section 3 discusses observational analyses. Section 4 investigates how AO influences winter Siberian high. Section 5 discusses the causes of winter sea–ice extent variations in the Barents Sea. Section 6 summarizes our findings along with a short discussion of some issues.

2. Dataset and methods

The dataset used in this study is from the National Centers for Environmental Prediction–National Center for Atmospheric (NCEP / NCAR) reanalysis dataset covering a 40–yr period from January 1958 to December 1997, including sea level pressure (SLP), 500 hPa height, nearly surface temperature at 2 m, and nearly surface wind fields at 10 m from ground, wind field and temperature field at each standard level from 200 to 1000 hPa.

In addition, we utilize monthly mean sea surface temperature (SST) for the period from January 1950 to December 1992 spanning $2^\circ \times 2^\circ$ in latitude and longitude, and monthly sea–ice concentration from 1953 to 1995, which taken from the web site: http: / / nsidc.org / NSIDC / CATALOG / data_ list_ by_ subject.html. The monthly mean volume flux (transport) of the North Atlantic seawater into the Barents Sea for the years of 1970–1994 (units: $Sv = 10^6$ m^3 s^{-1}) (across Fugloya–Bear Island section, i.e. the western entrance of the Barents Sea) and the monthly mean temperature of the upper 200 m of the water column from the Kola section (30°30′E) (the south shelf of the Barents Sea) are taken from Grotefemdt et al. (1998).

Because synoptic background at the earth surface is often influenced by steering flow aloft, we select the middle troposphere–500 hPa to define a new AO index. The new extent index of the winter (December–February) AO is defined as space gridpoint numbers at 500 hPa that are less than or equal to 5200 geopotential meters (hereafter AO index). This definition has many advantages: First, previous definitions about AO (NAO) mainly consider variations in SLP fields, but SLP is often influenced by land or oceanic boundary conditions. We also noticed that in SLP fields, AO (NAO) is more close to the North Atlantic sector. Second, it shows some problems to express AO variations by using the leading empirical orthogonal functions (EOF) modes of SLP. The leading modes only account for less than 50% of the total variance. Meanwhile, the calculation method is also inconvenient, i.e. it must utilize all of the historic dataset to obtain a new AO index. Finally, according to Wallace's opinion (Wallace 2000), the formation of AO is viewed as reflecting the interaction between the eddies and the zonally symmetric component of the flow, therefore, the definition of AO in the troposphere or the stratosphere is more reasonable.

In addition, a winter Siberian high (SH) extent index is also defined as space gridpoint numbers, which are greater than or equal to 1030 hPa on SLP in the Eurasian Continent.

As described in the introduction, strong northwesterlies prevails over the coast of East Asia during winter, while southwesterlies is dominant wind in summer. Therefore, the intensity of winter or summer monsoon of East Asia is closely tied with meridional wind, and further with temperature and rainfall. In this paper, an intensity index of the East Asian winter monsoon (EAWM) is defined as the sum of 13 normalized zonal SLP differences (110°E minus 160°E) over 20°–50°N with a 2.5° interval, which represents meridional wind component over the coast of East Asia. The sum is again normalized, namely (Shi et al. 1996):

$$M_t = \sum_{i=1}^{13} (A_{1it}^* - A_{2it}^*) ,$$

$$M_t^* = \frac{M_t - \overline{M}}{\sigma_M} .$$

where $\overline{M}$ and σ_M are the average and mean square deviation, respectively. A_{1it}^* and A_{2it}^* represent normalized (denoted by asterisk) SLP in the ith latitude and the tth year at 110°E and 160°E, respectively.

3. Observation analyses

3.1 *Interannual variations in winter SH, EAWM and winter AO*

Variations of intensity of EAWM greatly depend on behavior of both winter SH and Aleutian low. Actually, only using winter SH also can express intensity of EAWM. Variations of winter SH and EAWM (Fig. 1a) indicate that of them vary in–phase except for some special winters from 1963 / 1964 to 1965 / 1966 and 1968 / 1969, which represent significant discrepancy between them. Overall, stronger (weaker) EAWM corresponds to greater (smaller) extent of the winter SH. The correlation between the two time series is 0.46, exceeding 99% significant level. Conversely, variation of the winter AO is out–of–phase with winter SH (Fig. 1b). The simultaneous correlation is −0.56, also exceeding 99% significant level. Compared with Fig. 1a, variation of winter SH is more closely related to winter AO than to EAWM. This also shows that both winter SH and EAWM are obviously weak from the end of the

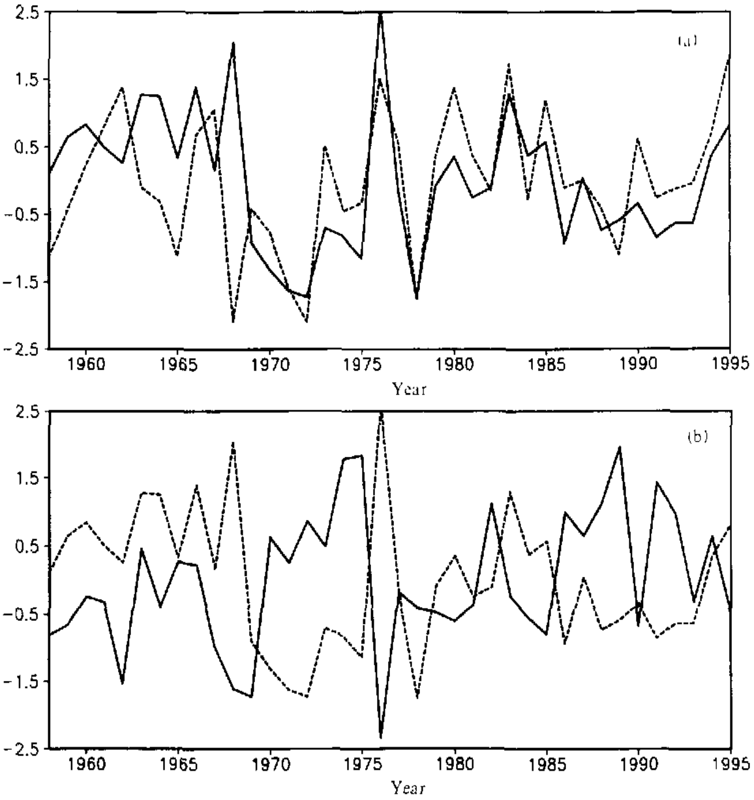

Fig. 1. (a) Variation of winter SH index (solid curve) and intensity index of EAWM (dashed curve). (b) Variation of winter AO index (solid curve) and winter SH index (dashed curve). All the data have been normalized.

1960's to the middle of the 1970's, while since 1990 both of them exhibited a upward trend.

AO, which exists throughout a year, is a perpetual center in the Northern Hemisphere, while winter SH only exists in winter (semi–perpetual active center in the atmospheric circulation). The interaction between the two active centers occurs in winter. If the interaction occurs, it would play the important rule in influencing climate variations over East Asia. To answer these questions, we perform the following analysis.

3.2 *Possible Influences of extremes in winter AO on climate over East Asia*

Based on the time series of winter AO, we selected five largest positive and five largest negative anomalies, respectively. The five largest positive anomalies include the winters of 1989 / 90, 1975 / 76, 1974 / 75, 1991 / 92 and 1988 / 89, and the largest negative anomalies are the winters of 1976 / 77, 1969 / 70, 1968 / 69, 1962 / 63 and 1967 / 68. Then, we perform composite and statistical significant test.

3.2.1 *SLP*

The predominant features (Fig. 2a) are that negative SLP differences appeared to the north of 55°N with its center being nearly in the north of Iceland and the east of Greenland. The negative maximum is less than −14 hPa. The negative SLP differences occupied much region controlled by SH, implicating weaker winter SH. Conversely, in middle latitudes positive SLP differences clearly have four positive centers. They are located in the middle and western Atlantic, Europe and the northern Africa, the eastern Tibetan Plateau, and the northern Pacific, respectively. Particularly in the northern Pacific, Europe and the northern Africa, positive SLP differences are even more remarkable. Obviously, winter Aleutian low is obviously weakened. Consequently, EAWM is weaker than normal. The regions where SLP differences are above the confidence level mainly include the entire Arctic and the northern Eurasia, Europe and the northern Africa, the middle–western North Atlantic, the northern Pacific. It is evident that the northern SH is weaker.

The distribution of SLP differences is very similar to the NAO. In this study, a winter NAO index is defined as the SLP differences at (40°N, 10°W) and (65°N, 22.5°W). It is similar to Hurrell's definition (1995) in which he used the normalized SLP difference between Lisbon, Portugal (38.8°N, 9.1°W) and Skykkisholmur, Iceland (65.1°N, 22.7°W). As suggested by Hurrel (1997), Ponta Delgada is a better station to describe the westward migration of the subtropical high through spring and summer. For winter season, however, Lisbon is an appreciate station compared to Ponta Delgada for defining the NAO index. The winter AO index is closely related to the NAO index as shown in Fig. 2b. The correlation coefficient between the two time series is 0.66, far exceeding 99.9% confident level, and further indicating that the AO and the NAO describe the same phenomenon. In addition, we also calculate correlations between winter AO index of this study and the simultaneous winter AO index

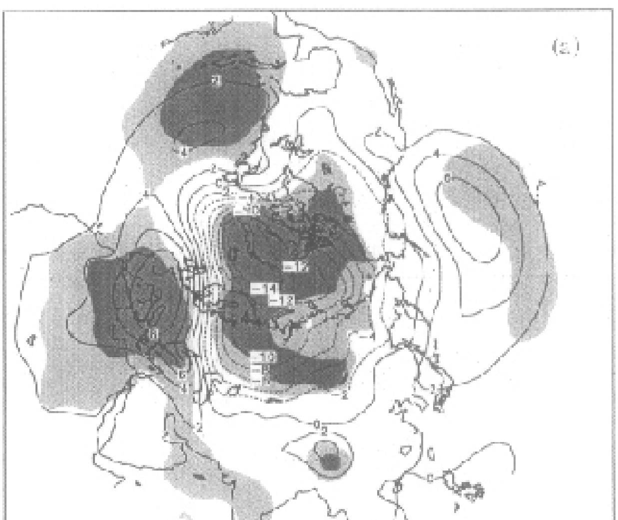

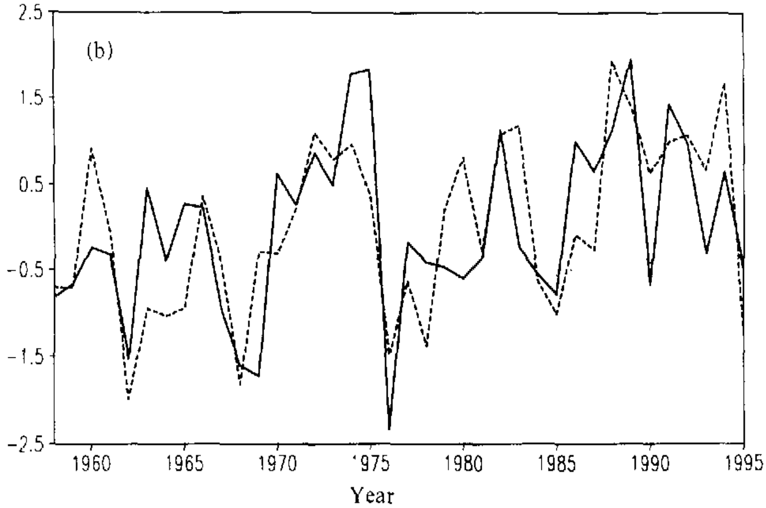

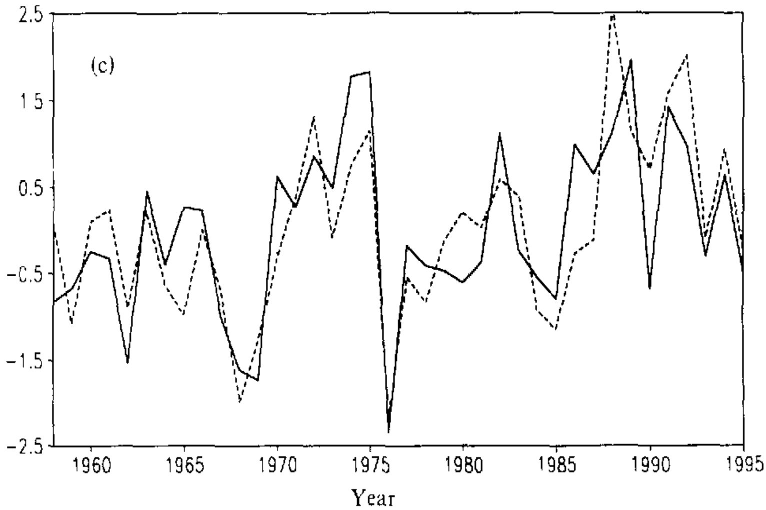

Fig. 2. (a) Differences in mean SLP between the two extremes in winter AO (the positive minus the negative), units: hPa. The heavy shaded area denotes the differences exceeding 99% confidence level, and the light is above 95% confidence level. (b) Variations of winter AO index (solid line) and the NAO index. (c) The same as in (b) except for Thompson and Wallace's AO index (dashed line). In (b) and (c), all the data have been normalized.

defined by Thompson and Wallace (1998). Figure 2c indicates that the two time series exhibit approximately the same trend; and the correlation coefficient is 0.77.

3.2.2 *Air temperature at 850 hPa*

The extreme change in winter AO not only influences SLP, but also affects air temperature. Figure 3 demonstrates that there are three warm centers in the Northern Hemisphere:

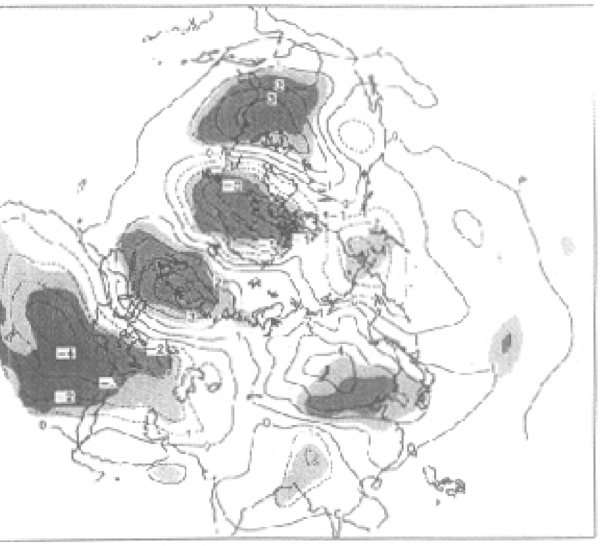

Fig. 3. Same as in Fig. 2a, except for air temperature (°C) at 850 hPa

one is the southern Canada and the middle–eastern United States; the second is the northern Europe and part of subarctic regions, such as the Barents Sea and the Kara Sea; the third is Siberia, Mongolia, the eastern China, Korea, Japan and the partly northwestern Pacific. Negative air differences appear in the following regions: the northeastern Canada and the entire Greenland with the largest negative temperature differences being nearby the Davis Strait and the Labrador Sea, the northern Africa and the western Asia, Alaska and the northeastern Russia. In general, corresponding to positive extremes in winter AO, air temperature is about 0.5–2°C higher than normal over East Asia, and about more than 2°C over the northern Asian Continent, while temperature over Alaska is about 1–3°C lower than normal. Conversely, for the negative extremes in winter AO air temperature over East Asia decreases by about 0.5–2°C and even exceeding 3°C over the north of 45°N. Alaska is 0.5–2°C higher. Another dominant feature of air temperature anomalies exhibits negative differences interval with the positive one. It seems to be like a structure of Rossby wave train. Significance test reveals that the regions surrounding the North Atlantic and the northern Africa are the most dominant. The northeastern Asia including Mongolia, China, Korea and Japan also shows stronger differences. The rest are Alaska, the eastern Tibetan Plateau and the northern Bay of Bengal. Undoubtedly, when winter AO is in its positive phase, air temperature over Mongolia, the eastern China, Korea and the southern Japan would be higher than normal.

3.2.3 *Geopotential height at 500 hPa*

Figure 4 shows that negative differences exceed 180 geopotential meters gpm over the southern Greenland. The largest positive difference occupies Europe. Over East Asia and the eastern United States, there are positive differences of above 60 gpm. Therefore, the trough is

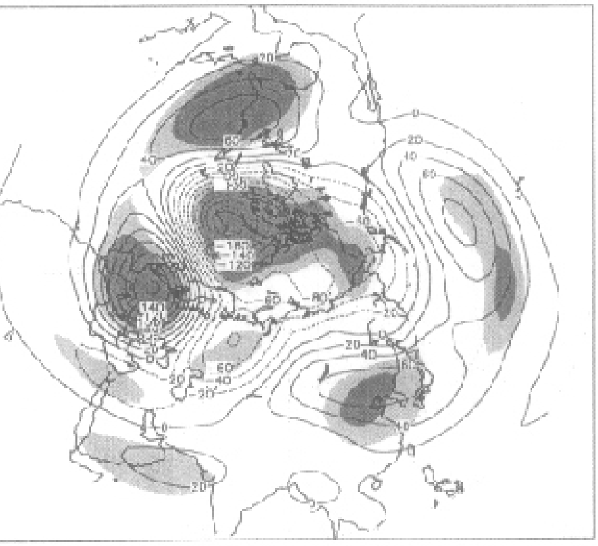

Fig. 4. Same as in Fig. 2a, except for geopotential height (gpm) at 500 hPa

weakened over East Asia. Consequently, cold wave attacking East Asia becomes inactive, implying weakened EAWM. Figure 4 also indicates that corresponding to AO's extreme positive phase, the extent of the polar vortex is notably reduced to north. The systems surrounding the polar vortex would move northward. Thus, there are positive height anomalies appearing in middle latitudes. Significance test also confirms that height differences over East Asia are above confidence levels. AO extremes show stronger influences over the western part of the Northern Hemisphere than East Asia and the northern Pacific. In fact, possible impacts from winter AO are not only restricted to some special extremes mentioned above, but also to universal AO events. Figure 5a represents correlations between winter AO and simultaneous SLP. There is significant negative correlation occupying the polar side of 50°N with positive correlations appearing in East Asia, and the northwestern and northern Pacific, implying that the northern SH is weaker. Correlations of winter AO with the nearly surface air temperature (2 m above ground) (Fig. 5b) exhibit the similar structure to Fig. 3. In Asia, the regions where correlations are positive and above 95% confidence level are mid-high latitudes in the Asia Continent, East Asia including China, Korea and the southern Japan, and the subtropical northern Pacific. Furthermore, positive correlations extend from the southern Japan to the South China Sea. In addition, positive correlations also cover the northern Europe and some subarctic regions, such as the Barents Sea, and the central and eastern United states. This phenomenon further demonstrates that the AO's positive phase directly results in higher air temperature appearing in East Asia and mid-high latitudes of the Asian Continent. Figure 5 reveals that winter AO is the most predominant system to control and influence interannual climate variability in the Northern Hemisphere, and its influences are even stronger than ENSO events.

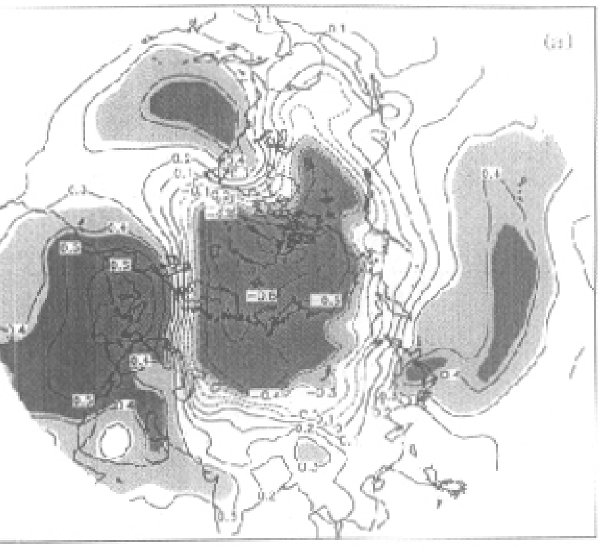

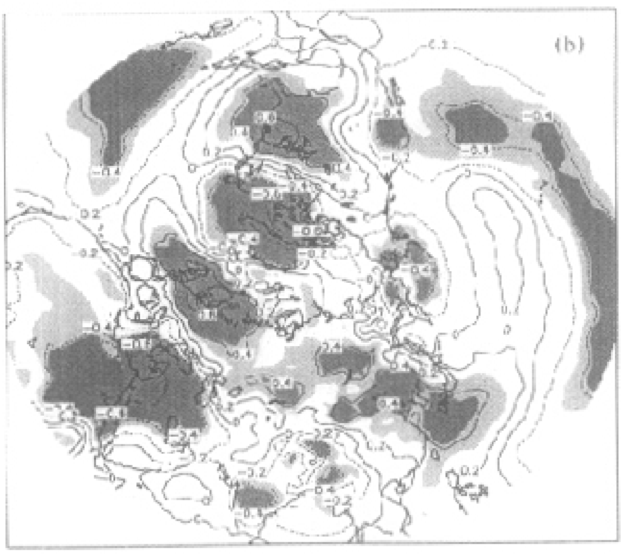

Fig. 5. Correlations of winter AO index with (a) winter SLP and (b) nearly surface air temperature at 2-meter high from the ground. The heavy shaded area represents that correlations exceed 99% confidence level, and the light is above 95% confidence level.

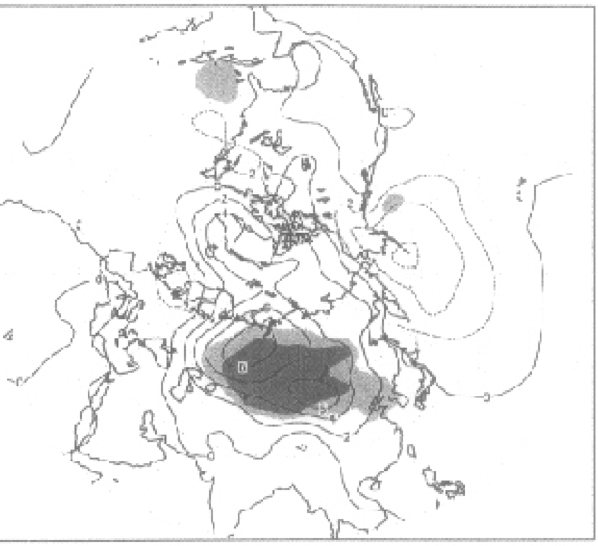

Fig. 6. Same as in Fig. 2a, except for winter SH. The positive extremes include the following winters: 1976 / 77, 1968 / 69, 1966 / 67, 1983 / 84, and 1963 / 64; and the negative are 1978 / 79, 1972 / 73, 1971 / 72, 1970 / 71, and 1975 / 76. The criterion for selecting those extremes is the same as in winter AO.

3.3 *Possible Influences of extremes in winter SH on SLP, 850 hPa temperature and geopotential heights at 500 hPa*

3.3.1 *SLP*

Compared with the negative phase of winter SH (Fig. 6), over most of Eurasia and entire Arctic, SLP notably rises with an largest increase appearing in the south to the Kara Sea, while in most of the northern Pacific SLP drops more than 6 hPa with its negative center being nearby the Alaska Peninsula. Consequently, winter Aleutian low deepens. It is evident that distribution of SLP differences is favorable for stronger EAWM. Winter AO seems to be weakened due to positive SLP differences in the entire Arctic region. Significance test indicates that the most significant differences in mean SLP appear in mid–high latitudes of the Asian Continent and East Asia. While in the entire Arctic and the northeastern North Atlantic, no significant differences exist, implying no dominant impact of extremes in winter SH on winter AO. Both the extent and intensity influenced by winter SH are obviously weaker than AO's influences (Fig. 2).

3.3.2 *Air temperature*

Differences of air temperature at 850 hPa between the two extremes in winter SH (Fig. 7) are negative over the mid–latitudes of the Asian Continent and the northwestern Pacific with

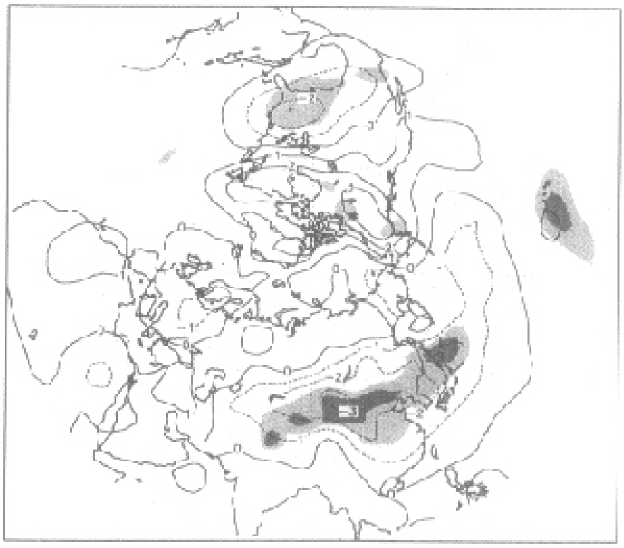

Fig. 7. Same as in Fig. 6, except for air temperature at 850 hPa.

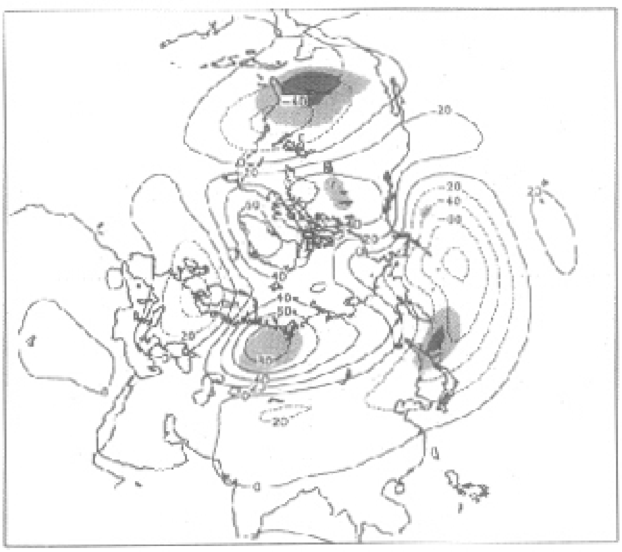

Fig. 8. Same as in Fig. 6, except for height at 500 hPa.

a negative largest value appearing in the southwest to the Lake Baykal. While over Alaska and the northwestern Canada, differences are positive. Significant test also confirms that temperature differences over the regions mentioned above exceed 95% confident levels. Therefore, Mongolia, China, Korea and Japan are mainly countries influenced by winter SH. When winter SH is in its positive phase, air temperature in those countries would drop, in response to a strong EAWM. We also notice no significant differences appearing in the Arctic region, implying no remarkable influences on winter AO.

3.3.3 *Geopotential height at 500 hPa*

The predominant feature (Fig. 8) is negative height differences covering most of middle latitudes in Asian Continent, East Asia, and the northwestern Pacific with a negative center appearing in the south of Aleutian. While nearly entire Arctic and part of high latitudes including the northern Eurasia and the northern America, the height differences are positive. The phenomenon clearly demonstrates that the trough over the northwestern Pacific would be deepened; and Aleutian low becomes stronger. Consequently, cold air activities over East Asia would be more active and frequent. Correspondingly, lower air temperature occurs in the regions. Significance test clearly indicates that extremes in winter SH exhibit no significant effects on winter AO.

4. How does the winter AO influence winter SH?

Using data analyses mentioned above, we found that winter AO significantly influences climate variations in East Asia, particularly through impacts on winter SH. The question is how the AO influences EAWM. Analyses in this study indicate that climate variations closely related to winter AO mainly occur in the western part of the Northern Hemisphere, Europe and the northern Africa. In other words, how do those anomalies far from East Asia influence winter SH, and further EAWM? It is widely known that 50°N latitude just crosses the body of winter SH. Thus, we first select the longitude–height section for u and w alone 50°N (Fig. 9). Upward motion (Fig. 9a) occupies nearly entire troposphere from 0 to 60°W (i.e. the North Atlantic sector) and the east of 140°E, while downward motion also controlls the entire troposphere from 20 to 40°E and 80 to 140°E. The latter is controlled only by winter SH. The phenomenon reveals that winter SH is closely related to dynamic processes, and further related to climate variations in the North Atlantic sector. Ding et al. (1991) also proposed that the maintaining of winter SH primarily depends on downward motion of airflow aloft. We notice that airflow also exhibits downward motion from 850 to 200 hPa in the region from 60 to 80°E. When winter AO is in its extremely positive phase (Fig. 9b, compared with Fig. 9a), streamlines from 60 to 80°E in nearly entire troposphere clearly show upward motion. Correlations between winter AO and vertical wind speed along 50°N show that positive correlations exceeding 95% confidence level cover nearly the entire troposphere of 60°–80°E and 30°–40°W, while negative correlations appears in 120°–140°E, 20°–40°E and 55°–70°W. This implies that the corresponding upward motion in the entire troposphere from 60 to 80°E is associated with the AO's positive phase. Conversely, when AO reaches its negative phase (Fig. 9c), airflow in the same region (i.e. from 60 to 80°E) shows strongly downward motion with the extent of downward motion increasing by more than 20 longitudes compared with Fig. 9b.

It is evident that variations of vertical motion (Fig. 9b) are even more violent than that in Fig. 9c. Upward motion is alternative with downward motion. Therefore, the circulation

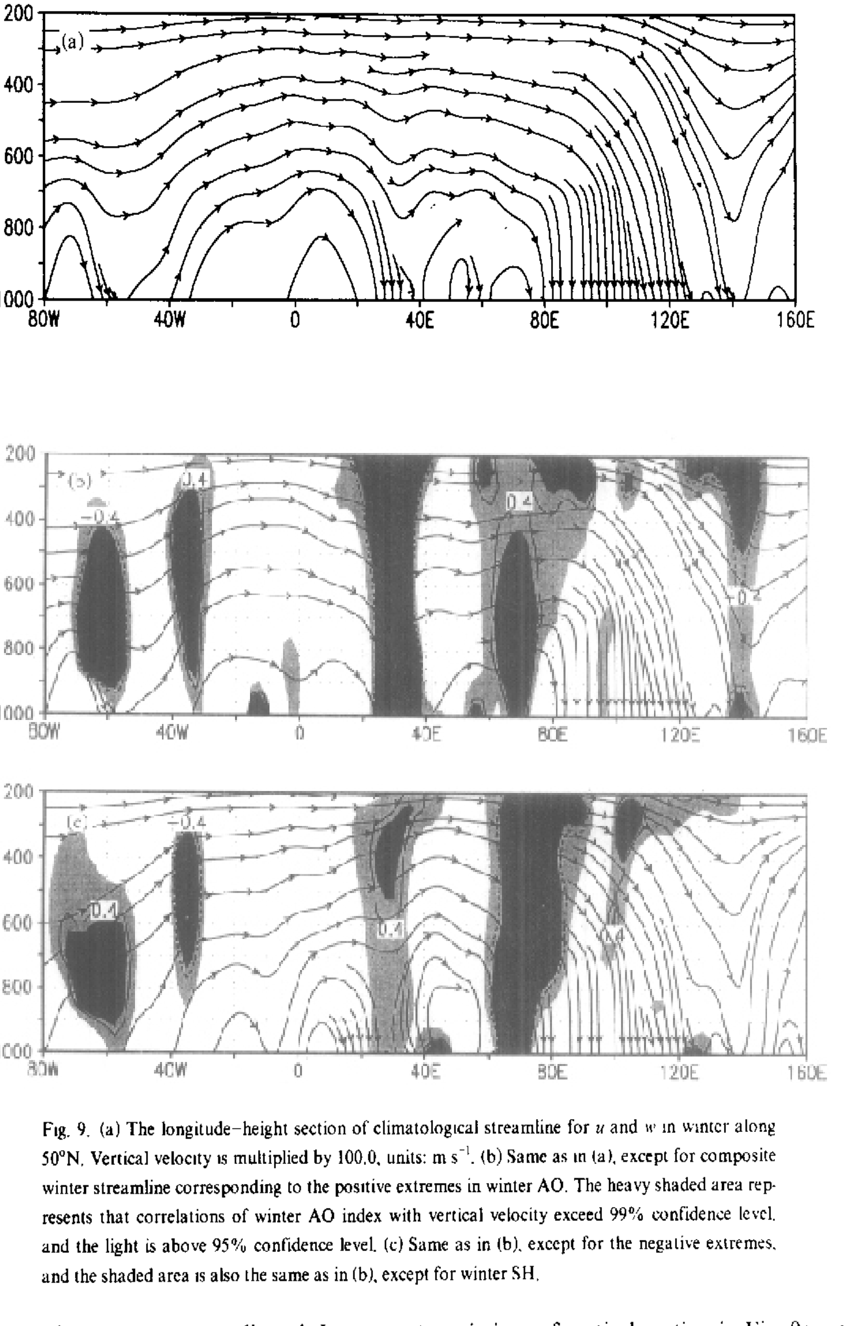

Fig. 9. (a) The longitude–height section of climatological streamline for u and w in winter along 50°N. Vertical velocity is multiplied by 100.0, units: m s^{-1}. (b) Same as in (a), except for composite winter streamline corresponding to the positive extremes in winter AO. The heavy shaded area represents that correlations of winter AO index with vertical velocity exceed 99% confidence level, and the light is above 95% confidence level. (c) Same as in (b), except for the negative extremes, and the shaded area is also the same as in (b), except for winter SH.

patterns become more complicated. In contrast, variations of vertical motion in Fig. 9c are simpler from 80°W to 140°E over the mid–high troposphere, i.e. the upward motion region from 80°W to about 40°E and the concurrent downward region appear in the region from 50 to 140°E over the mid–high troposphere. Correlations of winter SH with vertical wind speed

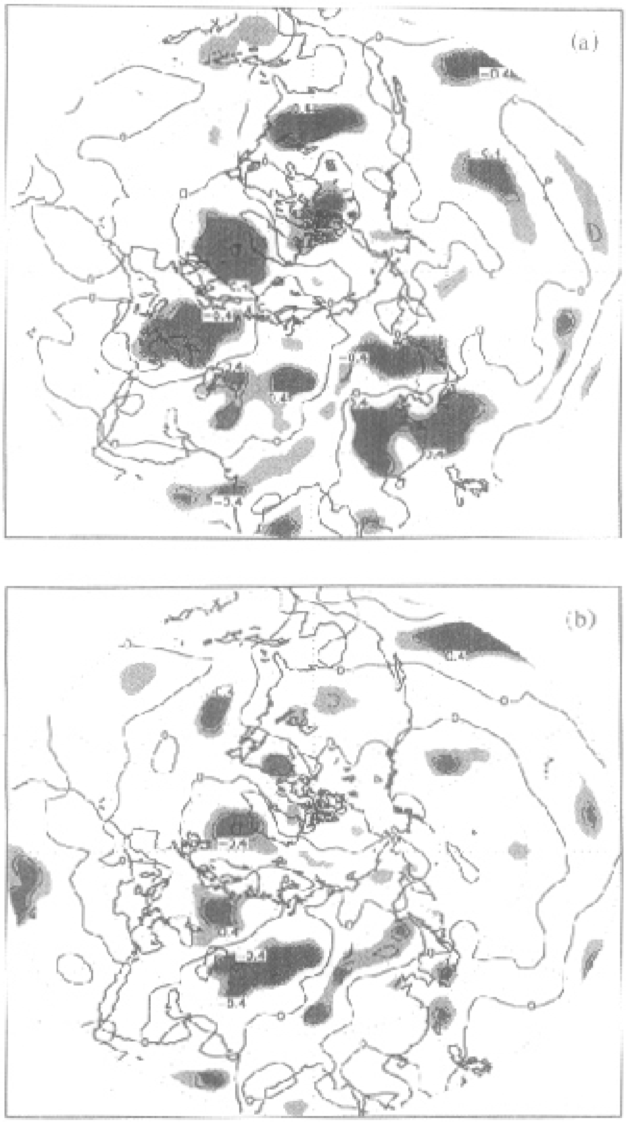

Fig. 10. (a) Correlations of winter AO index with vertical velocity at 200 hPa, and the shaded area is the same as in Fig. 9. (b) Same as in (a), but for winter SH.

also exhibit significant negative correlation over the same region. Undoubtedly, winter AO in fluences vertical motion, and further winter SH.

Above analyses clearly indicate that vertical motion in the whole troposphere is identical

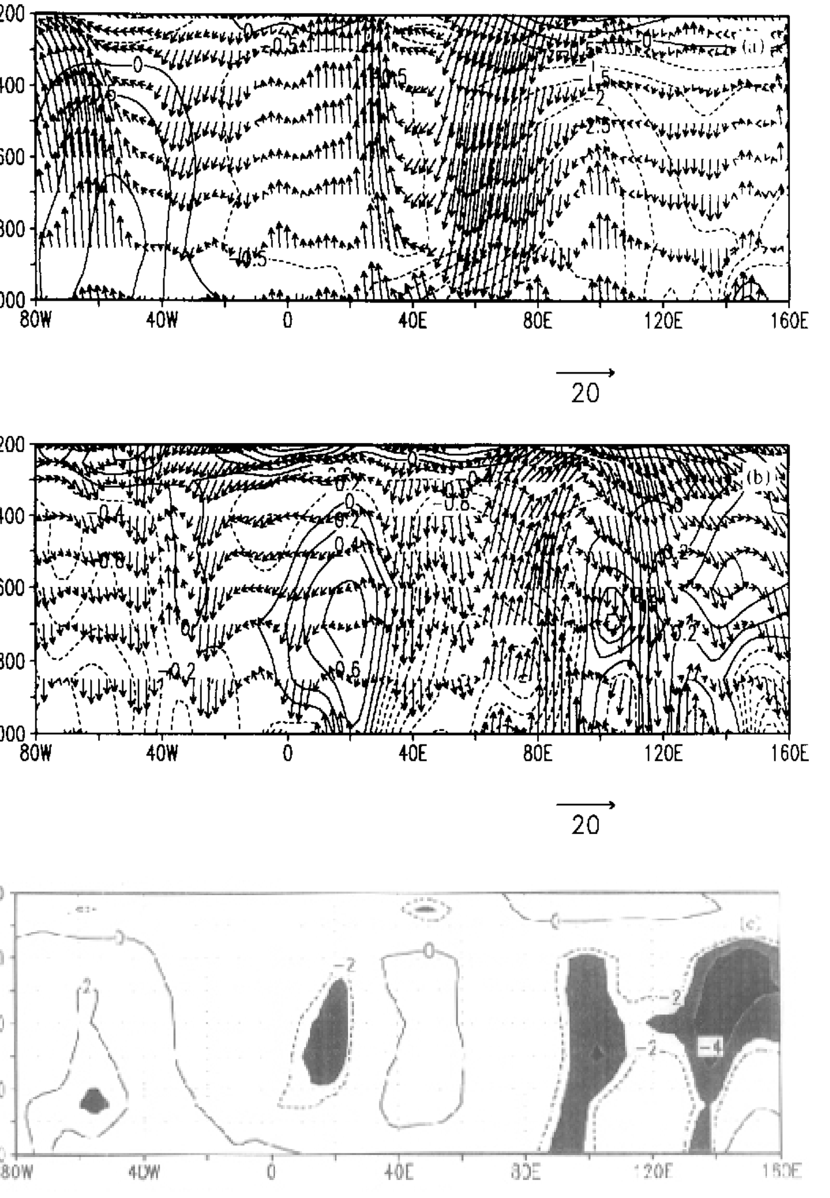

Fig. 11. The longitude-height section along 50°N of (a) composite anomaly wind field (u,w) (units: m s^{-1}) and anomaly air temperature (units: °C) according to the positive extremes in winter SH. Vertical velocity is multiplied by 1000.0. (b) Same as in (a), but for the negative extremes. (c) Significance test for differences in mean air temperature between the two extremes (the positive minus the negative). The shaded area is the same as in Fig. 2a.

(Fig. 9b, c), particular in 60°–80°E. So we select vertical motion at 200 hPa to represent the horizontal structures of the correlations between vertical motion and AO (SH) (Fig. 10). The predominant features shown in Fig. 10a are that distribution of correlations exhibits like Rossby wave train structure extending from the northern Canada southeastwards to the northwestern Pacific. The major positive correlation regions include the region between the eastern Greenland and the northwestern Europe, the central Eurasia, East Asia, and the northwestern Pacific. Consequently, when winter AO is in its positive anomalies, in East Asia from 20 to 40°N, the location occupied by the western SH and the north of Lake Balkhash the upward motion would become stronger, which directly diminishes extent of winter SH. This conclusion can be further confirmed from Fig. 10b.

The question is whether or not there is a close relation between vertical motion and air temperature over the region controlled by the winter SH. To explore the question, we select anomaly wind fields (u,w) and air temperature anomaly of the winter SH extremes. Figure 11a demonstrates that in response to positive extremes in winter SH, the largest downward motion anomalies also appear in the nearly same region, i.e. from 50 to 90°E, which is well consistent with Fig. 9c. We notice that weaker upward motion is over around 100°E, and speculate that the weaker upward motion anomalies are excited by stronger downward motion over both sides of it (anomaly downward motion is also evident in East Asia from 120 to 140°E). While for negative extremes in winter SH (Fig. 11b), anomalous downward motion controls the entire troposphere from 100 to 120°E, accompanied by upward motion anomalies appearing in 60–90°E. Compared to Fig. 11a, it is found that over the same region (i.e. from 60 to 80°E), although directions of anomalous vertical motion are opposite, they correspond to negative air temperature anomalies. Figure 11c shows the most significant differences of air temperature are located in the region from 130 to 150°E over the low–middle troposphere. Anomalous wind fields, however, do not exhibit any significant differences. Those phenomena demonstrate that vertical motion does not show any close relation with air temperature aloft.

As shown in Fig. 7, winter SH exhibits a close association with air temperature over the region from the central Asian Continent to East Asia. The further examination (Fig. 12) revealed that there is significant negative correlation appearing in the region from the Lake of Baykal to 25°N and from the Lake Balkhash to the northwestern Pacific with its center located in the regions from 35 to 50°N and from 90 to 120°N. Another predominant feature is the center of SLP does not coincide with the correlation's center; and the latter is located in

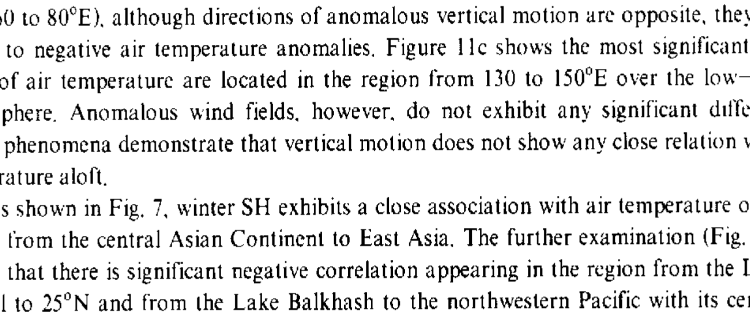

Fig. 12. Correlations of winter SH with air temperature at 850 hPa (the shaded area and the dashed line) and climatological mean SLP for winter. The shaded area is the same as in Fig. 11.

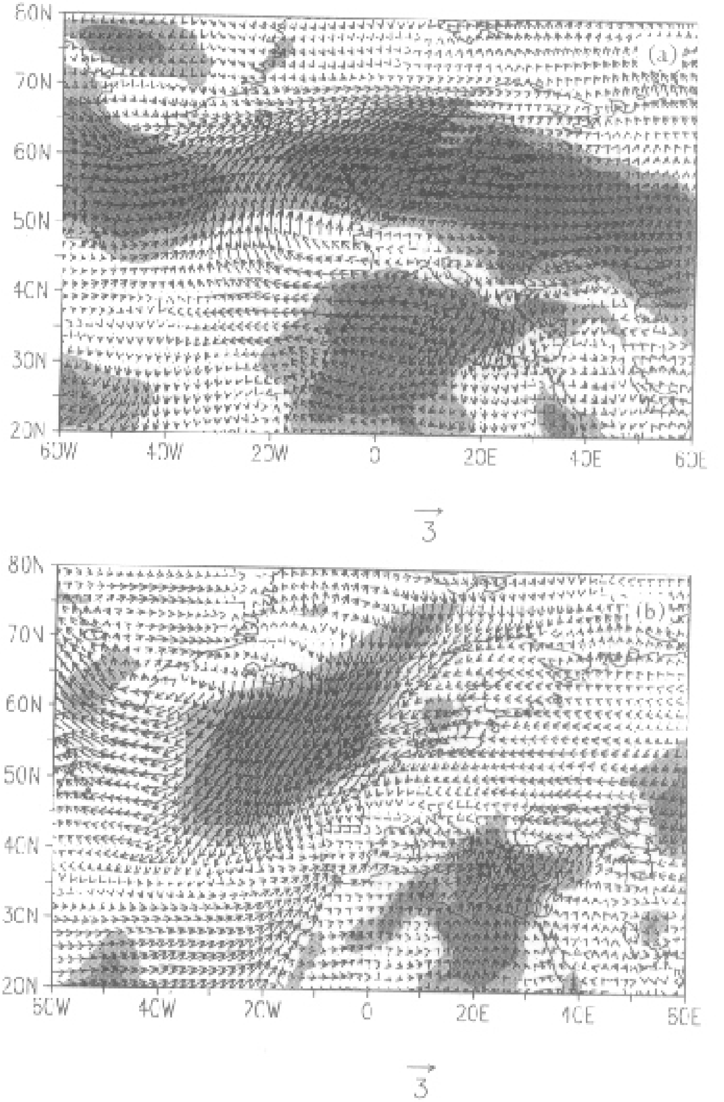

Fig. 13. (a) Composite of anomaly wind vector (m s^{-1}) at the nearly surface (10 m) in response to positive extremes in winter AO. The heavy shaded area represents that differences in mean u between the two extremes in winter AO (the positive minus the negative) exceed 99% confidence level, and the light is above 95% confidence level. (b) The same as in (a) but for the negative extremes and significance test for v.

the southeastern part of the former. If we consider correlations of winter SH with nearly surface air temperature, the correlation's center moves even southwards to the south of 45°N (not shown). Therefore, winter air temperature variations over the central Asian Continent East Asia are mainly influenced by winter SH. The lower temperature appearing in the southeastern SH results from cold airflow along the southwestern and southern SH.

5. Influences on winter sea–ice extent in the Barents Sea

Winter AO significantly influences not only atmospheric circulation over the North Atlantic, Arctic, and East Asia, but also Arctic sea–ice, especially on sea–ice extent in the North Atlantic (Dickson et al. 2000). Dickson et al. (2000), however, did not investigate the reasons for interannual variations of winter sea–ice extents in the Barents Sea, and they only stressed the median ice border at the end of April for the periods 1963–1969 and 1989–1995, corresponding, respectively, to minimum and maximum phases of the NAO index.

The influences of winter AO on the simultaneous sea–ice extent in the target region primarily depend on the following ways: the first is the surface wind–driven forcing; the second is the effect on transport of the North Atlantic Ocean warm water into the Barents Sea, further influencing seawater temperature.

Winter AO is closely associated with surface wind variations across the North Atlantic into Europe. There are strong southwesterly anomalies appearing in the northeastern North Atlantic (Fig. 13a), i.e. between Iceland and the northwestern Europe. In addition, southerly anomalies are overlying the Barents Sea, and directly contribute to decrease of sea–ice. The converse scenario can be observed (Fig. 13b) in response to negative phase of winter AO. We also notice that significant differences in mean westerly and southerly between the two extremes in winter AO just occur in the northeastern North Atlantic. Driven by surface wind forcing, the warm current would transport more warm seawater into polar region via the

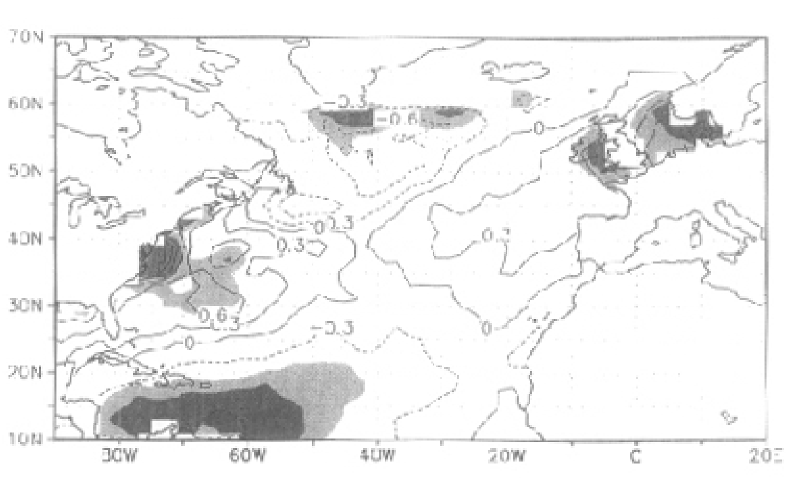

Fig. 14. Differences in mean SST (°C) between the two extremes in winter AO (the positive minus the negative). The shaded area is the same as in Fig. 2a.

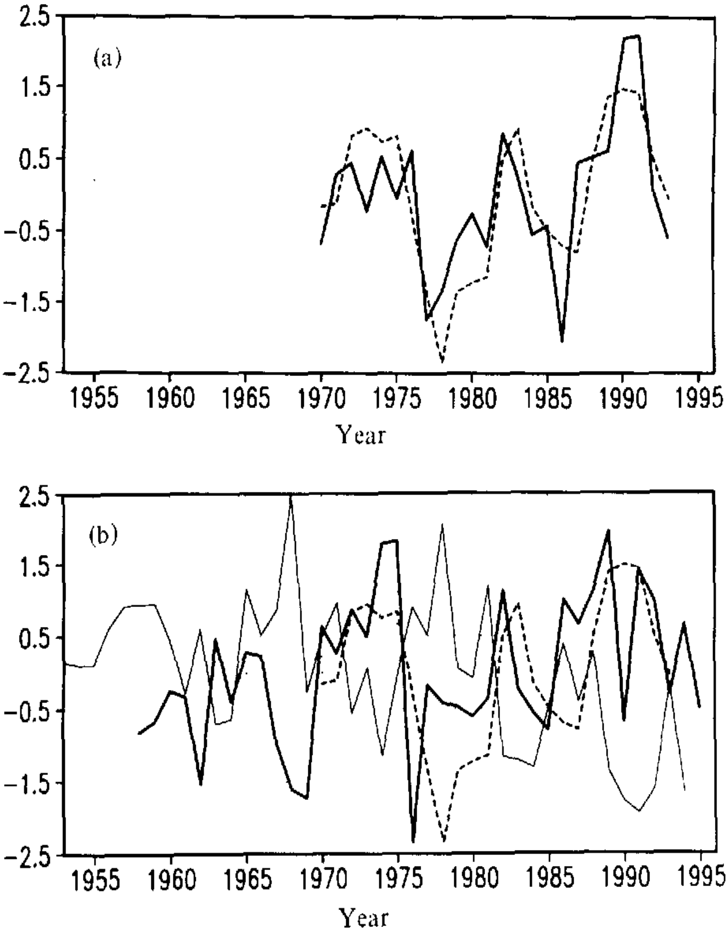

Fig. 15. (a) Winter seawater volume fluxes across the FuglΦya–Bear Island section at the western entrance of the Barents Sea (solid line) and the simultaneous temperature of upper 200 m of the water column from Kole section (33°30′E) (dashed line). (b) Winter AO index (thick solid line) and winter sea–ice extent index in the Barents Sea (thin solid line) and mixed layer seawater temperature (dashed line). All the data have been normalized. Note: the data shown in (a) are taken from Grotefendt et al. (1998), and for Fugloya–Bear Island section and Kole section see the Fig. 1 in Grotefendt et al. (1998).

Barents Sea in response to positive extremes in winter AO. Actually, influenced by AO, SST is obviously higher in the eastern and northeastern Atlantic (Fig. 14). Significance test for SST differences also confirms that along the eastern Atlantic coast, SST differences exceed 95% confident level.

The following observation (Fig. 15) further confirms our speculations. The winter mean seawater volume fluxes into the Barents Sea are closely related to the simultaneous mean seawater temperature of upper 200 m (Fig. 15a). More Atlantic seawater inflow causes higher temperature in the mixed layer with the correlation coefficient being 0.74. The winter AO index is also closely related to seawater temperature (Fig. 15b) with the correlation coefficient being 0.49, implying that high AO phase would transport more North Atlantic seawater into the Barents Sea, and further raises seawater temperature. Therefore, seawater temperature would influence sea–ice coverage. Figure 15b clearly indicates the inverse relation between seawater temperature and sea–ice extent.

6. Conclusions and discussions

This paper has aimed to identify climate signatures over East Asia and the winter sea–ice extent in the Barents Sea in response to winter AO. The following conclusions are drawn:

(1) Winter AO exhibits the predominant influences on climate variations over East Asia. When winter AO is in its positive (negative) phase, SLP significantly falls (rises) in high latitudes and entire Arctic. The concurrent positive (negative) SLP anomalies appear in the nearly entire middle latitudes of the Northern Hemisphere, and positive (negative) air temperature anomalies occupy East Asia. As a result, both winter SH and EAWM are weaker (stronger) than normal.

(2) The maintaining of winter SH primarily depends on downward motion of airflow aloft, greater part of which originates from the North Atlantic sector. Winter SH variation has close association with the vertical motion variation in the nearly entire troposphere over its western part, i.e. the west of 90°E and the north of Lake Balkahsh.

(3) Winter AO possibly influences winter SH in the following manners: first, SLP directly decreases (increases) in high latitudes of the Asian Continent. The other is that winter AO influences the vertical motion, and further influences winter SH. When winter AO shows its positive anomalies, the vertical motion becomes stronger over the middle–low latitudes of the East Asia and the region between 90°E and the Caspian Sea from 45 to 55°N.

(4) Winter SH only influences climate in the central Asian Continent and East Asia, whose effects exhibit "the local features" compared with AO. Winter SH has no significant influences on Arctic climate. Variations of EAWM greatly depend on behavior of both winter SH and Aleutian low. Actually, winter SH variations also approximately represent variations of EAWM. In general, strong winter SH directly results in low temperature over the central Asian Continent, East Asia, and part northwestern Pacific, leading to strong EAWM.

(5) By means of influencing surface wind stress, surface sea temperature and the transport of the North Atlantic warm seawater into subarctic, particularly into the Barents Sea, the winter AO variations further influence the simultaneous sea–ice extent in the Barents Sea.

In the light of those analyses investigated above, we obtain further understanding of climate in the Northern Hemisphere in response to winter AO. AO is not limited in Arctic and the North Atlantic sector. Actually, the winter AO anomaly exhibits close associations with the climate anomaly in the Northern Hemisphere, even with the global climate system. Our preliminary research clearly indicates that the winter AO anomaly is closely related to the previous anomaly climate signals occurring in middle–low latitudes. The anomaly signals gradually move northwards to Arctic (not shown). This phenomenon implies that anomalous climate in middle low latitudes may be the leading factors for creating the winter AO anomaly. Therefore, it is necessary to further examine possible physical mechanisms for the winter AO anomaly and its influences on climate over East Asia, particularly for its associations with teleconnection as shown in Fig. 10a and Fig. 3.

In addition, we should also emphasize the important roles of the ocean (including sea–ice coverage) on atmospheric circulation (Wu et al. 1999). Figure 9a clearly demonstrates that over the North Atlantic sector and the northern Pacific (east of 140°E) the upward motion occupies nearly entire troposphere, signifying the oceanic heating plays the crucial roles.

REFERENCES

Baldwin, M. P., X. Cheng, and T. J. Dunkerton, 1994: Observed correlation between winter mean tropospheric and stratospheric circulation anomalies. *Geophys. Res. Lett.*, **21**, 1141–1144.

Barnston, A. G., and R. E. Livezey, 1987: Classification, seasonally, and persistence of low–frequency atmospheric circulation patterns. *Mon. Wea. Rev.*, **115**, 1083–1126.

Cayan, D. R., 1992a: Latent and sensible heat flux anomalies over the northern oceans: The connection to monthly atmospheric circulation. *J. Climate*, **5**, 354–369.

Cayan, D. R., 1992b: Variability of latent and sensible heat fluxes estimated using bulk formulae. *Atmos. Ocean*, **30**, 1–42.

Cayan, D. R., 1992c: Latent and sensible heat flux anomalies over the northern oceans: Driving the sea surface temperature. *J. Phys. Oceanogr.*, **22**, 859–881.

Cayan, D. R., and G. Reverdin, 1994: Monthly precipitation and evaporation variability estimated over the North Atlantic and North Pacific. *Proc. Atlantic Climate Change Program: PIs' Meeting*, Princeton, NJ, NOAA, 28–32.

Chen, W., H.–F. Graf, and Huang, R.–H., 2000: The interannual variability of East Asian Winter Monsoon and its relation to the summer monsoon. *Advances in Atmospheric Sciences*, **17**(1), 48–60.

Deser, C., 2000: On the teleconnectivity of the "Arctic oscillation". *Geophys. Res. Lett.*, **27**(6), 779–782.

Dickson, R. R., T. J. Osborn, J. W. Hurrell, J. Meincke, J. Blindheim, B. Adlandsvik, T. Vinje, G. Alekseev, and W. Maslowski, 2000: The Arctic Ocean response to the North Atlantic Oscillation. *J. Climate*, **13**, 2671–2696.

Ding, Y., S. Wen, and Y. Li, 1991: A study of dynamic structures of the Siberian high in winter. *Acta Meteorologica Sinica*, **49**(4), 430–439.

Fyfe, J. C., G. J. Boer, and G. M. Flato, 1999: The Arctic and Antarctic oscillation and their projected changes under global warming. *Geophys. Res. Lett.*, **26**(11), 1601–1604.

Gao D., and Wu B., 1998: A preliminary study on decadal oscillation and its oscillation source of sea–ice–air system in the Northern Hemisphere. *Polar Meteorology and Glaciology*, **12**, 68–78.

Grotefendt, K., K. Logemann, D. Quadfasel, and S. Ronski, 1998: Is the Arctic Ocean warming? *J. Geophys. Res.*, **103**(C12), 27679–27687.

Hansen, D. V., and H. F. Bezdek, 1996: On the nature of decadal anomalies in the North Atlantic sea surface temperature. *J. Geophys. Res.*, **101**, 9749–9758.

Hurrell, J. W., 1995: Decadal trends in the North Atlantic Oscillation: Regional temperatures and precipitation. *Science*, **269**, 676–679.

Hurrell, J. W., 1996: Influence of variations in extratropical wintertime teleconnections on Northern Hemisphere temperature. *Geophys. Res. Lett.* **23**, 665–668.

Hurrell, J. W., and H. Van Loon, 1997: Decadal variations in climate association with the North Atlantic Oscillation. *Climatic Change*, **36**, 301–326.

Ji L., Sun S., and K. Arpe, 1997: Model study on the interannual variability of Asian winter monsoon and its influence. *Advances in Atmospheric Sciences*, **14**, 1–22.

Kang, I., and Y. Jeong, 1996: Association of interannual variations of temperature and precipitation in Seoul with principal modes of Pacific SST. *J. Korean Meteor. Soc.*, **32**, 339–345.

Kitoh, A., H. Koide, K. Kodera, S. Yukimoto, and A. Noda, 1996: Interannual variability in the stratospheric–tropospheric circulation in a ocean–atmosphere coupled GCM. *Geophys. Res. Lett.*, **23**, 543–546

Kodera, K., M. Chiba, H. Koide, A. Kitoh, and Y. Nikaidou, 1996: Interannual variability in the winter stratosphere and troposphere in the Northern Hemisphere. *J. Meteor. Soc. Japan*, **74**, 365–382

Lau, K.-M., 1992: The East Asian summer monsoon rainfall variability and climate teleconnection. *J. Meteor. Soc. Japan*, **70**, 211–241.

Lau, K.-M., and M. Li, 1984: The monsoon of East Asia and its global association– A survey. *Bull. Amer. Meteor. Soc.*, **65**, 114–125

Myers, R. A., J. Helbig, and D. Holland, 1989: Seasonal and interannual variability of the Labrador Current and West Greenland Current. ICES CM Mimeo 1989 / C: 16, 18pp.

Mysak, L. A, R. G. Ingram, J. Wang, and A. V. D. Baaren, 1996: The anomalous sea–ice extent in Hudson Bay, Baffin Bay and the Labrador Sea during three simultaneous NAO and ENSO episodes. *Atmosphere Ocean*, **34**(2), 313–343.

Mysak, L. A., and Venegas, 1998: Decadal climate oscillations in the Arctic: A new feedback loop for atmosphere–ice–ocean interactions. *Geophys. Res. Lett.*, **25**(19), 3607–3610.

Perlwitz, J., and H.-F. Graf, 1995: The statistical connection between tropospheric and stratospheric circulation of the Northern Hemisphere in winter. *J. Climate*, **8**, 2281–2295.

Rogers, J. C., 1984: The association between the North Atlantic Oscillation and the Southern Oscillation in the Northern Hemisphere. *Mon. Wea. Rev.*, **12**, 1999–2015.

Serreze, M. C., F. C. Carse, R. G. Barry, and J. C. Roger, 1997: Icelandic low cyclone activity climatological features, linkages with the NAO, and relationships with recent changes in the Northern Hemisphere circulation. *J. Climate*, **10**, 453–464.

Skeie, P., 2000: Meridional flow variability over the Nordic seas in the Arctic Oscillation ramework. *Geophys. Res. Lett.*, **27**(16), 2569–2572.

Slonosky, V. C., L. A. Mysak, and J. Derome, 1997: Linking Arctic sea–ice and atmospheric circulation anomalies on interannual and decadal timescales. *Atmosphere Ocean*, **35**, 333–366.

Shi N., Lu J., and Zhu Q., 1996: The intensity index of winter and summer monsoon over East Asia and its variation. *J. Nanjing Institute of Meteor.*, **19**, 168–176 (in Chinese)

Tao S., and Zhang Q., 1998: Response of the East Asian summer monsoon to ENSO events. *Acta Atmos. Sinica*, **22**, 399–407 (in Chinese).

Tomita, T., and T. Yasunari, 1996: Role of the northeast winter monsoon on the biennial oscillation of the ENSO monsoon system. *J. Meteor. Soc. Japan*, **74**, 399–413

Thompson, D. W., and J. M. Wallace, 1998: The arctic oscillation signature in the wintertime geopotential height and temperature fields. *Geophys. Res. Lett.*, **25**, 1297–1300.

Walker, G. T., 1923: Correlation in seasonal variations of weather, VIII: A preliminary study of world weather. *Mem. Ind. Meteor. Dept. (Poona)*, **24**, 275–310.

Wallace, J. M., 2000: North Atlantic Oscillation / annular mode: Two paradigms–one phenomenon. *Quart. J. Roy. Meteor. Soc.*, **126**(564), 791–805.

Walsh, J. E., and C. M. Johnson, 1979: An analysis of Arctic sea ice fluctuations, 1953 to 1977. *J. Phys. Oceanogr.*, **9**, 580–591.

Wang, B., Wu R., and X. Fu, 2000: Pacific–East Asian Teleconnection: How Does ENSO affect Asian Climate? *J. Climate*, **13**, 1517–1536.

Wang, J., V. D. Baaren, and L. A. Mysak, 1995: A principal component analysis of gridded sea–level pressure, surface air temperature, and sea–ice concentration of the arctic region, 1953–1993. C2GCR Rep. No. 95–4, McGill Univ., 18pp + figures +Fortran programs. (available at the International Arctic Research Center, University of Alaska Fairbanks: jwang@iarc.uaf.edu).

Wang, J., and M. Ikeda, 2000: Arctic Oscillation and Arctic sea–ice oscillation. *Geophys. Res. Lett.* **27**(9), 1287–1290.

Wang, J., L. A. Mysak, and R. G. Ingram, 1994: Interannual variability of sea–ice cover in Hudson Bay, Baffin Bay and the Labrador Sea. *Atmosphere Ocean*, **32**, 421–447.

Wu B., Gao D., and Huang R., 1997: ENSO events and interannual variations of winter sea–ice in the Greenland the Kara and the Barents Seas. *Chinese Science Bulletin*, **42**(16), 1382–1385.

Wu B., Huang R., and Gao D., 1999: The impact of variations of winter sea–ice extents in the Kara Barents Seas on winter monsoon over East Asia. *Acta Meteor. Sinica*, **13**, 141–153.

Yasunari, T., 1991: The monsoon year–A new concept of the climatic year in the Tropics. *Bull. Amer. Meteor. Soc.*, **72**, 937–957.

Zhang, R., A. Sumi, and M. Kimoto, 1996: Impact of El Nino on the East Asian monsoon: A diagnostic study of the '86/87 and '91/91 events. *J. Meteor. Soc. Japan*, **74**, 49–62.

冬季北极涛动对西伯利亚高压、东亚冬季风以及海冰范围的可能影响

武炳义　王　佳

P4　A

摘　要

利用 NCEP/NCAR 月平均再分析资料(1958–1997)，月平均海表面温度资料(1950–1992)以及月的海冰密集度资料(1953–1995)，研究了冬季北极涛动与西伯利亚高压、东亚冬季风以及巴伦支海海冰范围之间的联系。研究结果表明，冬季北极涛动不仅影响北极和北大西洋区域气候变化，并且可能影响冬季西伯利亚高压，进而影响东亚冬季风。当冬季北极涛动处于正位相时，冬季西伯利亚高压和东亚冬季风都偏弱，在西伯利亚南部和东亚沿岸、包括中国东部、韩国和日本，从地表面到对流层中部气温偏高 0.5–2°C。当冬季北极涛动处于负位相时，结果正相反。研究结果还表明，冬季西伯利亚高压对北极以及北大西洋区域气候变化没有显著的影响，与北极涛动的影响相比，西伯利亚的影响强度和范围明显偏弱。研究进一步揭示了冬季北极涛动可能影响西伯利亚高压的可能机理。冬季西伯利亚高压与动力过程以及从地表面到对流层中部的气温变化有密切的关系。西伯利亚高压的西部变化主要依赖于动力过程，而其东部与气温变化更为密切。冬季西伯利亚高压的维持主要依赖于对流层中的下沉气流，这种下沉气流源于北大西洋区域，其变化受到北极涛动的影响。当冬季北极涛动处于正(负)位相时，气流的下沉运动明显减弱(增强)，进而影响冬季西伯利亚高压。此处，冬季北极涛动对同时期的巴伦支海海冰范围有显著的影响。

关键词：北极涛动，西伯利亚高压，东亚冬季风，海冰范围